JACC: BASIC TO TRANSLATIONAL SCIENCE VOL. 4, NO. 1, 2019

PRECLINICAL RESEARCH

Bioactive Materials Facilitating Targeted Local Modulation of Inflammation

Richard P. Tan, MSc,[a,b,*] Alex H.P. Chan, BSc,[a,b,*] Simon Wei, PhD,[c] Miguel Santos, PhD,[a,d] Bob S.L. Lee, MSc,[a,b] Elysse C. Filipe, PhD,[b,e] Behnam Akhavan, PhD,[a,d,f] Marcela M. Bilek, PhD, MBA,[d,f,g,h] Martin K.C. Ng, MBBS, PhD,[b,i] Yin Xiao, PhD,[c] Steven G. Wise, PhD[a,b]

VISUAL ABSTRACT

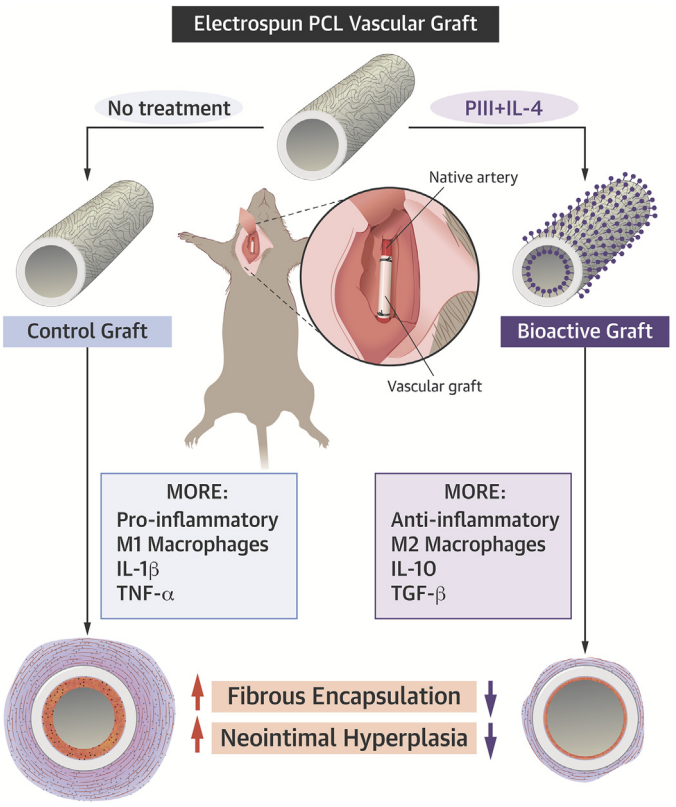

Tan, R.P. et al. J Am Coll Cardiol Basic Trans Science. 2019;4(1):56–71.

HIGHLIGHTS

- **Electrospun polycaprolactone surfaces were immobilized with a monolayer of the cytokine interleukin-4 to create a "bioactive" immunomodulatory surface capable of influencing the phenotype of macrophages responding to the material surface in vivo.**
- **Bioactive surfaces, evaluated in vitro by using macrophage culture, exhibited upregulation of anti-inflammatory M2 genes and facilitated morphological changes consistent with macrophage activation.**
- **As a subcutaneous implant in a 14-day model of acute inflammation, bioactive surfaces polarized macrophages from their M1 pro-inflammatory to M2 anti-inflammatory phenotypes, leading to a significant reduction in the local immune-driven foreign body response.**
- **As vascular grafts in a 28-day mouse carotid interposition model, bioactive grafts maintained their macrophage polarization and immunomodulatory effects, significantly reducing adventitial encapsulation and neointimal hyperplasia development.**

From the [a]Heart Research Institute, Sydney, New South Wales, Australia; [b]Sydney Medical School, University of Sydney, Sydney, New South Wales, Australia; [c]Science and Engineering Faculty, Queensland University of Technology, Brisbane, Queensland, Australia; [d]School of Physics, University of Sydney, Sydney, New South Wales, Australia; [e]Garvan Institute of Medical Research, Cancer Division, Sydney, New South Wales, Australia; [f]School of Aerospace, Mechanical and Mechatronic Engineering, University of Sydney, Sydney, New South Wales, Australia; [g]Charles Perkins Centre, University of Sydney, Sydney, New South Wales, Australia; [h]Sydney Nano Institute, University of Sydney, Sydney, New South Wales, Australia; and the [i]Royal Prince Alfred Hospital, Sydney, New South Wales, Australia. *Mr. Tan and Dr. Chan contributed equally to the manuscript and are joint first authors. This work was supported by the Australian Research Council (Dr. Bilek) and the National Health and Medical Research Council (APP1066174; Dr. Ng). Mr. Tan, Mr. Lee, and Dr. Filipe are recipients of an Australian Postgraduate Scholarship, and

ISSN 2452-302X https://doi.org/10.1016/j.jacbts.2018.10.004

SUMMARY

Cardiovascular disease is an inflammatory disorder that may benefit from appropriate modulation of inflammation. Systemic treatments lower cardiac events but have serious adverse effects. Localized modulation of inflammation in current standard treatments such as bypass grafting may more effectively treat CAD. The present study investigated a bioactive vascular graft coated with the macrophage polarizing cytokine interleukin-4. These grafts repolarize macrophages to anti-inflammatory phenotypes, leading to modulation of the pro-inflammatory microenvironment and ultimately to a reduction of foreign body encapsulation and inhibition of neointimal hyperplasia development. These resulting functional improvements have significant implications for the next generation of synthetic vascular grafts.

ABBREVIATIONS AND ACRONYMS

CAD = coronary artery disease

ELISA = enzyme-linked immunoadsorbent assay

IL = interleukin

PCL = polycaprolactone

PIII = plasma immersion ion implantation

qPCR = quantitative polymerase chain reaction

TGF = transforming growth factor

TNF = tumor necrosis factor

The role of inflammation in the genesis and progression of coronary artery disease (CAD) and other manifestations of atherosclerosis has long been established (1). Inflammatory cells drive the initial stages of plaque formation, express growth factors and cytokines that progress disease, and can worsen patient outcomes after an acute coronary syndrome (2). The recent CANTOS (Canakinumab Anti-inflammatory Thrombosis Outcome Study) trial showed that systemic administration of canakinumab, a selective antibody against the inflammatory cytokine interleukin (IL)-1β, significantly lowered the incidence of recurrent cardiovascular events (3). By systemically reducing inflammation while having no effect on lipid levels, CANTOS was a large-scale clinical trial showing that pharmaceutical anti-inflammatory therapy was effective in reducing cardiovascular events. Although these results will have a significant impact on the immediate direction of therapeutic interventions, systemic canakinumab treatment was associated with a higher risk of fatal infection and sepsis, most likely resulting from sustained global immune suppression. Accordingly, future translation of therapies for the treatment of CAD based on anti-inflammatory approaches will benefit from local, targeted modulation of inflammation.

The severity and extent of host foreign body immune responses toward cardiovascular interventional devices significantly affect their long-term performance. The modification of implantable medical devices using anti-inflammatory surface coatings has been previously explored (4). The most effective strategies rely on the controlled release of anti-inflammatory agents to halt local inflammatory responses in the surrounding tissue. Dexamethasone is a commonly used synthetic glucocorticoid hormone shown to reduce the levels of tumor necrosis factor (TNF)-α, IL-1β, IL-6, and interferon gamma. α-Melanocyte-stimulating hormone is a linear peptide shown to reduce TNF-α levels while increasing anti-inflammatory IL-10 levels. Previous controlled-release strategies using anti-inflammatory agents typically involved nonspecific, passive diffusion through polyelectrolyte layers, biodegradable coatings, or swelling coatings. Although these approaches have led to a reduction in some aspects of the foreign body response, including protein adsorption and cell adhesion in vitro, complications such as recurrent inflammatory responses and subsequent device replacement may potentially arise when drug elution is complete. Furthermore, nonspecific blockade of immune cell recruitment after elution of anti-proliferative drugs, as is the case for drug-eluting stents, can impair the resolution of chronic inflammation and hinder long-term device integration and function (5). Improved application of these strategies would therefore aim to better retain the bioactivity, stability, and residence time of locally delivered agents while more selectively modulating the

Mr. Chan and Dr. Santos have received funding support from the Heart Research Institute. The authors acknowledge the financial support of E. Brackenreg. The authors have reported that they have no relationships relevant to the contents of this paper to disclose.

All authors attest they are in compliance with human studies committees and animal welfare regulations of the authors' institutions and Food and Drug Administration guidelines, including patient consent where appropriate. For more information, visit the *JACC: Basic to Translational Science* author instructions page.

Manuscript received August 10, 2018; revised manuscript received October 10, 2018, accepted October 12, 2018.

immune response to facilitate prolonged functional benefits.

We have identified macrophages and their broad spectrum of phenotypes as master effectors of the foreign body response toward implanted materials. At the 2 ends of the spectrum are the M1 (pro-inflammatory) and M2 (anti-inflammatory) phenotypes, which regulate a host of inflammatory cytokines to either propagate or halt innate inflammation, respectively. Modification of the material surface to induce the M2 phenotype of responding macrophages may potentially represent an effective means of mitigating foreign body responses to implanted materials.

In the present study, we developed a novel off-the-shelf bioactive device coating for local and lasting modulation of the inflammatory response to implants. A plasma immersion ion implantation (PIII) surface treatment was used that facilitates the rapid covalent attachment of biomolecules while preserving their bioactivity (6). One of the most well-established and highly documented biomolecules responsible for M2 macrophage phenotype polarization is the cytokine IL-4 (7). Bioactive signaling chemokines such as IL-4 have not previously been immobilized on material surfaces without chemical linkers, representing a fundamentally new off-the-shelf approach to local regulation of inflammation. Herein we examined the in vitro behavior of macrophages in response to bioactive IL-4 surfaces before assessing the in vivo inflammatory responses in 2 distinct mouse models. Comprehensive immunohistochemical analysis of both subcutaneous and carotid arterial graft implants was used to quantitatively assess macrophage phenotype, local cytokine expression, and measures of functional outcome (including fibrous encapsulation and neointimal hyperplasia).

METHODS

PIII SURFACE TREATMENT. Surface modification of electrospun polycaprolactone (PCL) scaffolds was conducted by using PIII as previously described (8). Briefly, nitrogen was admitted into a custom-built vacuum chamber to a working pressure of 2×10^{-3} Torr, and plasma discharges were generated by inductively coupled radiofrequency power at a frequency of 13.56 MHz. Scaffolds were placed on an electrically biased stainless-steel holder. Ion acceleration was achieved through application of -20 kV pulses with a temporal width of 20 μs at a frequency of 50 Hz, drawing a current of 1.3 mA. PIII treatment was run for 800 s, providing ion fluences of 1×10^{16} ions/cm^2. Characterization methods of PIII-treated surfaces can be found in the Supplemental Methods.

BIOACTIVE IL-4 SURFACE CREATION. For in vitro experiments, scaffolds were biopsy punched into 5-mm diameter circular discs and placed into Eppendorf tubes. Recombinant mouse IL-4 (2 μg/ml in sterile phosphate-buffered saline) was added to each scaffold for 1 h at room temperature. To test IL-4 attachment, scaffolds were washed in sodium dodecyl sulfate (5% in phosphate-buffered saline) for 4 h at room temperature before enzyme-linked immunoadsorbent assay (ELISA) using an anti-IL-4 monoclonal antibody (Thermo Fisher Scientific, Waltham, Massachusetts) and horseradish peroxidase-conjugated secondary antibody (Abcam, Cambridge, Massachusetts). For in vivo experiments, both flat scaffolds and PCL conduits (0.5 mm diameter) were incubated in recombinant mouse IL-4 (2 μg/ml in sterile phosphate-buffered saline) for 1 h at room temperature and rinsed in sterile phosphate-buffered saline before implantation.

In vivo performance of bioactive IL-4 subcutaneous implants. Study approval was obtained from the Sydney Local Heath District Animal Welfare Committee (protocol number 2013/050). Experiments were conducted in accordance with the Australian Code of Practice for the Care and Use of Animals for Scientific Purpose. Mice were given four 1.5-cm incisions (two rows side-by-side) on their dorsal surfaces to create subcutaneous pockets, as previously described (9). Scaffolds were then inserted into each pocket (5 mice per time point equaling 5 scaffolds per group per time point) and sutured closed by using 6-0 silk sutures. Explants were taken at 3, 7, and 14 days' post-implantation; analysis is detailed in the Supplemental Methods.

In vivo performance of bioactive IL-4 vascular grafts. Study approval was obtained from the Sydney Local Heath District Animal Welfare Committee (protocol number 2015/016). Experiments were conducted in accordance with the Australian Code of Practice for the Care and Use of Animals for Scientific Purpose. C57/BL6 mice (male, 9 to 10 weeks old, 25 ± 2 g) were purchased from Australian BioResources (Moss Vale, NSW, Australia). Vascular grafts (5 per group) were implanted into the carotid artery by using a previously described technique (10). Briefly, the right common carotid artery was double ligated, and polyimide cuffs (Cole-Parmer North America, Vernon Hills, Illinois) were placed around each end. Overhanging arteries were everted on the plastic cuff, and grafts were then sleeved over each end and secured with 8-0 sutures. Clamps were removed, and blood flow was confirmed with pulsation. After 28 days, mice were perfused with heparinized saline (50 U/ml), and the grafted carotid artery

was isolated and dissected proximal and distal to the graft. Analysis of the vascular cross-sections is detailed in the Supplemental Methods.

RESULTS

CREATION OF A NOVEL IL-4–IMMOBILIZED BIOMATERIAL SURFACE. Control surfaces were PIII treated in nitrogen plasma for a duration of 800 s. Energetic ions accelerated by the 20-kV negative bias penetrate through the scaffold surface, breaking chemical bonds along their path and displacing atoms in the polymer structure. This results in a highly crosslinked, dense, carbonized structure at the surface of the scaffold (**Figure 1A**). The high density of broken bonds and displaced atoms allow for creation of new bonds (**Figure 1B**). The unpaired electrons that remain manifest as reactive radical groups (**Figure 1C**) embedded in the treated layer that gradually diffuse to the surface via thermally activated, local restructuring (Supplemental Results). Radical diffusion leads to surface oxidation, allowing direct covalent immobilization of IL-4 upon contact with the scaffold surface (6). Mechanical testing of scaffolds (n = 6 each group) exhibited no significant differences in Young's modulus or strain after PIII treatment (Supplemental Figure 1).

Bioactive IL-4 surfaces were created by incubating the PIII-treated surfaces in an IL-4 solution (2 μg/ml) for 1 h at room temperature (**Figure 1D**). Robust, covalent immobilization was shown by washing surfaces in sodium dodecyl sulfate (5%) for 4 h at room temperature to remove any passively adsorbed molecules (11,12), followed by IL-4 quantification using ELISA (n = 3 each group) (**Figure 1E**). Although the PIII-treated scaffolds retained IL-4 (bioactive IL-4), IL-4 was completely removed from the untreated PCL surfaces (passive IL-4).

BIOACTIVE IL-4 SURFACES MODULATE MACROPHAGE PHENOTYPE IN VITRO. RAW264.7 murine macrophages were seeded onto bioactive IL-4 surfaces to evaluate macrophage polarization (**Figure 2A**), as commonly reported (13–15). Macrophage morphology and material interaction were first characterized by using scanning electron microscopy. At 8 h post-seeding, cells cultured on bioactive IL-4 surfaces appeared more spread, with a notably rougher cell surface (**Figure 2B**). Cytoskeletal morphologies, observed by using confocal microscopy, further showed strikingly different morphology. Expression of M2 phenotype genes, arginase-1, CD163, CD206, and IL-10 revealed that passive IL-4 surfaces enhanced the expression of only arginase-1 and IL-10 but had no significant effect on CD163 or CD206. Similarly, PIII-only surfaces significantly increased arginase-1 expression but not the other markers. Only bioactive IL-4 surfaces significantly increased all marker expression at 8 h post-seeding compared with control (**Figure 2C**). These results show that IL-4 covalently immobilized on PIII-treated surfaces robustly polarizes macrophages toward an M2 phenotype and demonstrates that this immobilization approach is necessary for sustained bioactivity.

BIOACTIVE IL-4 SUBCUTANEOUS IMPLANTS REDUCE INFLAMMATORY CYTOKINES AND FIBROUS ENCAPSULATION. A 14-day subcutaneous mouse back model of acute inflammation was initially used to evaluate the in vivo functionality of bioactive IL-4 surfaces (16) (5 scaffolds per group) (**Figure 3A**), before further evaluation in a vascular context. Immunostaining markers for total macrophages ($CD68^+$), M1 (major histocompatibility complex Class II), and M2 (CD206) phenotypes were used to assess macrophage responses (**Figure 3B**). Increasing macrophage recruitment, observed on control surfaces, was reduced by 79 ± 6% and 86 ± 7% on bioactive IL-4 surfaces at days 7 and 14, respectively (**Figure 3B**, top). Bioactive IL-4 surfaces also increased M2 macrophage polarization by 159 ± 11% at day 3, suggesting earlier M2 polarization compared with control (**Figure 3B**, middle). Bioactive IL-4 surfaces also exhibited a 360 ± 15% higher M2/M1 macrophage ratio at day 14 compared with control, indicating a predominantly M2 phenotype residing at the implant surface in the late phases post-implantation (**Figure 3B**, bottom). These results were observed in representative images illustrating a large accumulation of macrophages on control surfaces with a predominantly M1 phenotype. In contrast, bioactive IL-4 surfaces exhibited a significant reduction in total macrophage accumulation and an enhancement of the M2 phenotype (**Figure 3C**).

To corroborate these findings, quantitative polymerase chain reaction (qPCR) and ELISA analysis for classic M1 and M2 markers were conducted at days 3 and 7 post-implantation to assess gene and protein expression changes, respectively. qPCR results revealed that bioactive implants had significantly less TNF-α and inducible nitric oxide synthase at day 3 (Supplemental Figure 2A) and the ELISA results showed significantly reduced IL-1β and IL-6 in bioactive implants at days 3 and 7 (Supplemental Figure 2B). These results were consistent with our immunohistochemistry and validated the presence of a robust anti-inflammatory microenvironment surrounding bioactive subcutaneous implants by independently demonstrating an upregulation of M2 markers and a downregulation of M1 markers.

FIGURE 1 **Characterization of PIII Treatment on PCL Control Surfaces**

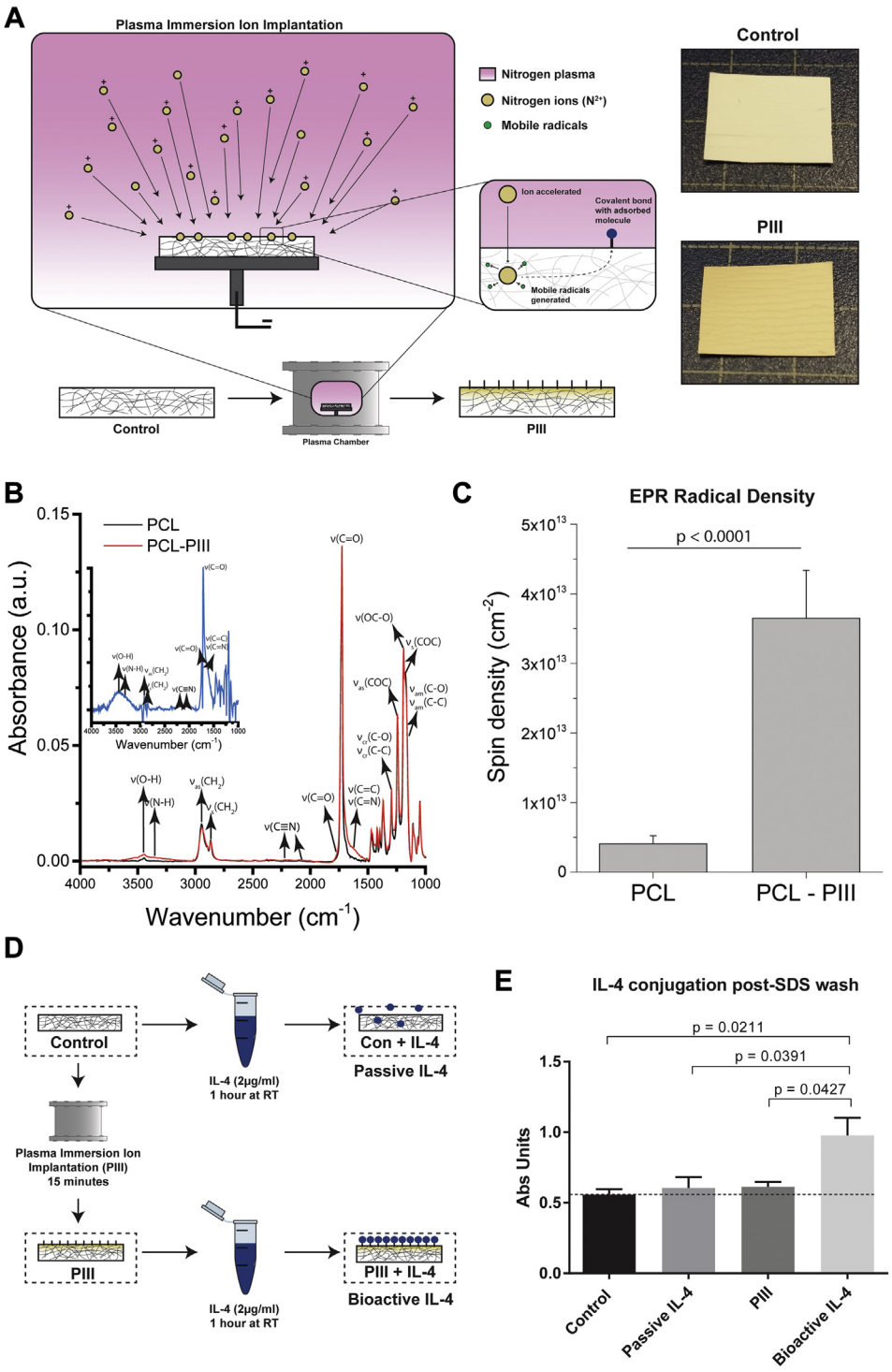

(A) Plasma immersion ion implantation (PIII) schematic with representative images of control surfaces before **(top)** and after **(bottom)** treatment. **(B)** Attenuated total reflectance Fourier-transform infrared spectroscopy (ATR FT-IR) surface characterization. **(C)** Electron paramagnetic resonance (EPR) characterization. **(D)** Diagram of experimental groups. **(E)** Interleukin-4 (IL-4) retention enzyme-linked immunoadsorbent assay (n = 3 per group). PCL = polycaprolactone; RT = room temperature; SDS = sodium dodecyl sulfate.

FIGURE 2 **In Vitro Biofunctionality of IL-4 Bioactive Surfaces**

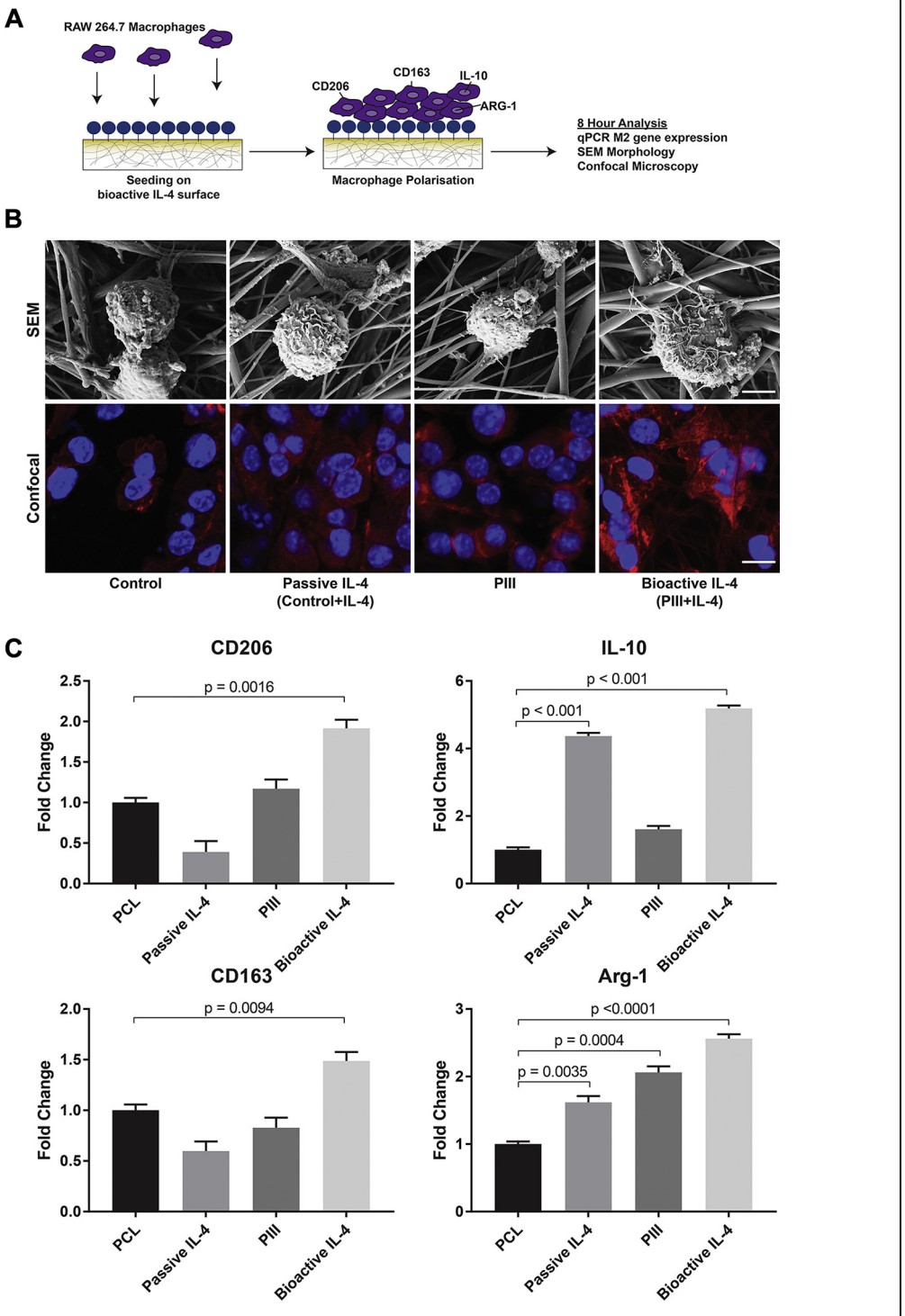

(A) Schematic of experimental design. **(B)** Scanning electron microscopy (SEM) (top row; scale bar represents 50 μm) and confocal microscopy (bottom row; scale bar represents 5 μm) of cultured macrophages. **(C)** Quantitative polymerase chain reaction (qPCR) of M2 Phenotype genes (n = 5 per group). Abbreviations as in Figure 1.

FIGURE 3 Implantation of Bioactive IL-4 Surfaces in Subcutaneous Mouse Model

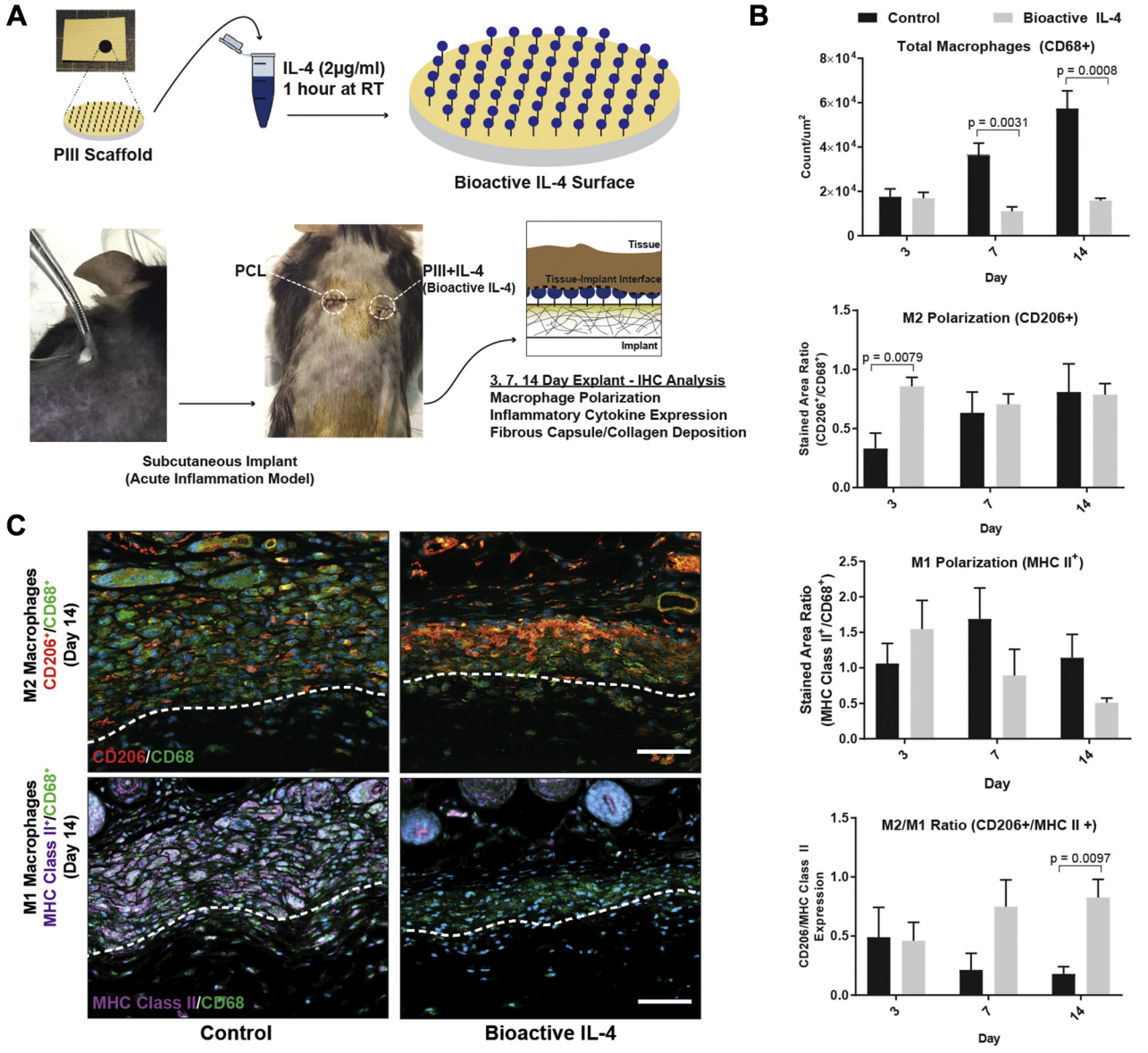

(A) Experimental design schematic. **(B)** Immunohistological quantification of macrophages at the implant surface: total $CD68^+$ macrophages **(top)**, $CD206^+$ M2 polarization **(middle)**, and M2/M1 ($CD206^+$/ major histocompatibility complex (MHC) Class II^+) ratio **(bottom)**. **(C)** Representative images of M2 **(top row)** and M1 **(bottom row)** macrophages. CD68 stained in **green**, CD206 stained in **orange**, and MHC Class II stained in **purple**. **Dotted lines** represent the interface between tissue **(above)** and implant **(below)**. Scale bar represents 60μm; n = 5 per group. IHC = immunohistochemical; other abbreviations as in Figure 1.

Further immunohistochemical analysis was conducted to confirm the expression of inflammatory cytokines (5 scaffolds per group). IL-10 and transforming growth factor (TGF)-β were chosen as classic anti-inflammatory cytokines, whereas IL-1β and TNF-α are well-characterized pro-inflammatory cytokines (17). Bioactive IL-4 surfaces increased IL-10 expression by 432 ± 26% at day 7 compared with controls (Figure 4A). TGF-β expression was also increased 1025 ± 11% at day 7 on bioactive IL-4 surfaces. Representative images show this increased IL-10 and TGF-β present at the scaffold/tissue interface in bioactive surfaces (Figure 4B). Corresponding changes to classically pro-inflammatory cytokines occurred at later time points, with significant differences at day 14. IL-1β and TNF-α

FIGURE 4 **Inflammatory Cytokine Quantification at the Implant Surface In Vivo**

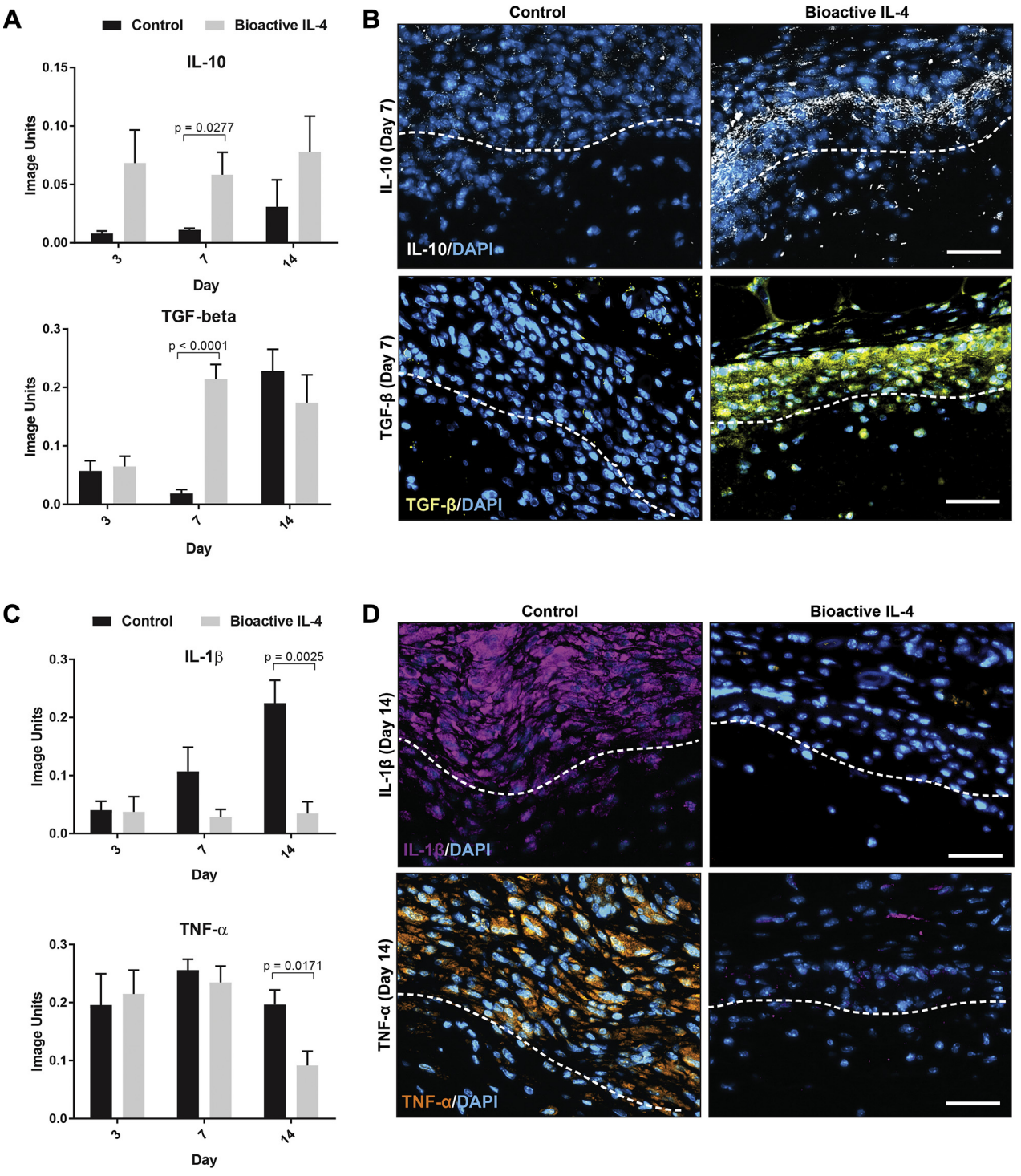

(A) Immunohistological quantification of anti-inflammatory cytokines IL-10 **(top)** and transforming growth factor (TGF)-β **(bottom)**. **(B)** Representative images of IL-10 **(top)** and TGF-β **(bottom)** expression at the implant surface stained in **white** and **yellow** respectively. **(C)** Immunohistological quantification of pro-inflammatory cytokines IL-1β **(top)** and tumor necrosis factor (TNF)-α **(bottom)**. **(D)** Representative images of IL-1β **(top)** and TNF-α **(bottom)** expression at the implant surface stained in **purple** and **orange** respectively. **Dotted lines** represent the interface between tissue **(above)** and implant **(below)**. Scale bar represents 40 μm; n = 5 per group. Abbreviations as in Figure 1.

FIGURE 5 Functional Outcomes of Bioactive IL-4 Surfaces In Vivo

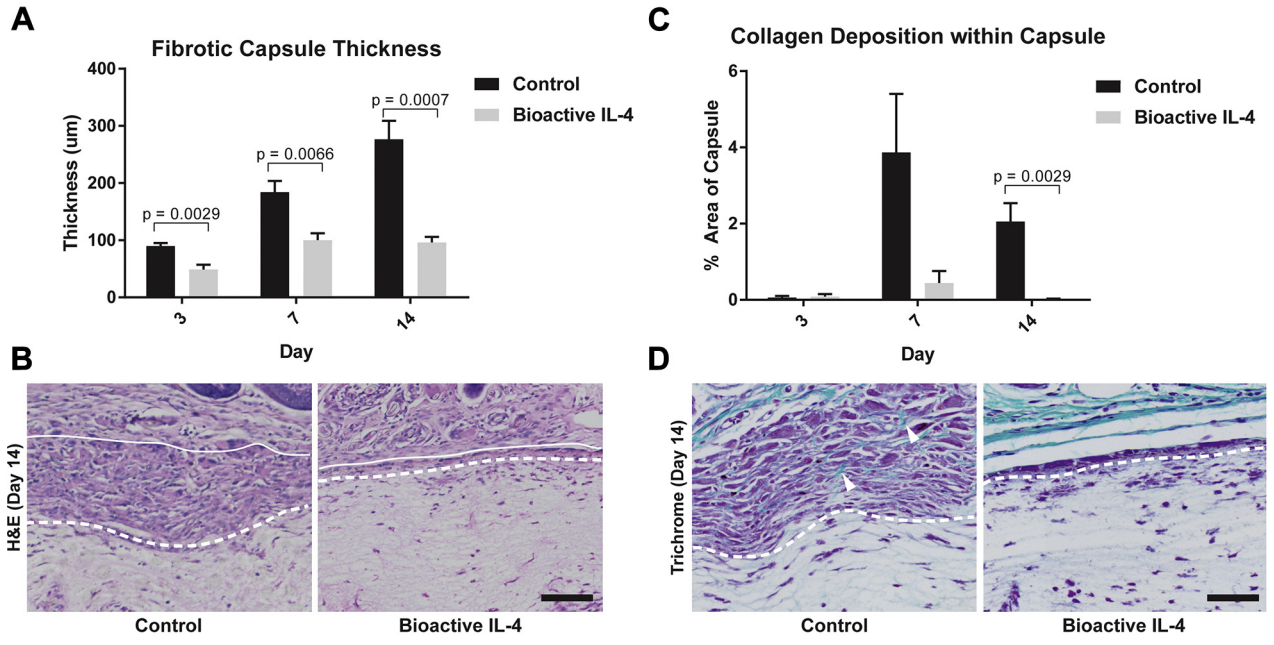

(A) Measurement of fibrotic capsule formation/thickness at the implant surface **(top)**. **(B)** Representative hematoxylin and eosin (H&E) stains of fibrotic capsules. **(C)** Quantification of collagen deposition at the implant surface. **(D)** Representative trichrome stains of collagen **(green)** within the fibrotic capsule, highlighted by **arrows**. **Dotted lines** represent the interface between tissue **(above)** and implant **(below)**. Scale bar represents 50 μm, n = 5 per group. IL-4 = interleukin 4.

expression was 84 ± 7% and 53 ± 5% less, respectively, on bioactive IL-4 surfaces compared with control (Figure 4C). Again, representative images clearly show these striking changes at the material interface where bioactive IL-4 implants seem to all drastically reduce IL-1β and TNF-α (Figure 4D).

We next sought to characterize functional changes arising from an increased proportion of M2 macrophages and positive regulation of local cytokine production. The fibrotic capsule thickness for the control implants increased steadily over time, as expected, from 90 ± 5.1 μm at day 3 to 276.6 ± 132.1 μm by day 14 (Figure 5A). In contrast, the capsule thickness on bioactive IL-4 surfaces was reduced at all time points with a final reduction of 65 ± 4% at day 14, compared with control, evident in representative images (Figure 5B). Furthermore, peak collagen deposition in PCL controls occurred at day 7 comprising 3.8 ± 2% of the capsule area, with less (2.0 ± 0.7%) by day 14 (Figure 5C). In bioactive IL-4 surfaces, collagen was reduced at day 7 with a significant reduction at day 14, as seen in representative images (Figure 5D). Reductions in collagen deposition over time further suggest significant modulation of the host foreign body response.

BIOACTIVE IL-4 SYNTHETIC ARTERIAL GRAFTS REDUCE LOCAL INFLAMMATION AND NEOINTIMAL HYPERPLASIA. Small diameter vascular grafts were manufactured with bioactive IL-4 surfaces on both the luminal and adventitial surfaces, implanted into an established mouse carotid interposition grafting model, and explanted at 28 days (Figure 6A). Consistent with results from the subcutaneous implant study, IL-4 grafts significantly reduced total macrophages present by 54 ± 6% compared with control (Figure 6B). These macrophages also showed a 47 ± 12% increase in the M2 phenotype and a corresponding decrease in the M1 phenotype by 52 ± 9%, demonstrating similar macrophage polarization effects. This outcome was further supported by a 93 ± 11% increase in the M2/M1 ratio of bioactive IL-4 grafts compared with control. These changes are highlighted in representative images, showing fewer total macrophages and enhanced expression of CD206 with less major histocompatibility complex class II (Figure 6C).

Further examination revealed that anti-inflammatory IL-10 and TGF-β levels were significantly increased by 122 ± 11% and 539 ± 35%, respectively, in bioactive IL-4 grafts compared with controls (Figures 7A and 7B). In addition,

FIGURE 6 **Investigation of IL-4 Bioactive Surfaces for Synthetic Vascular Grafts**

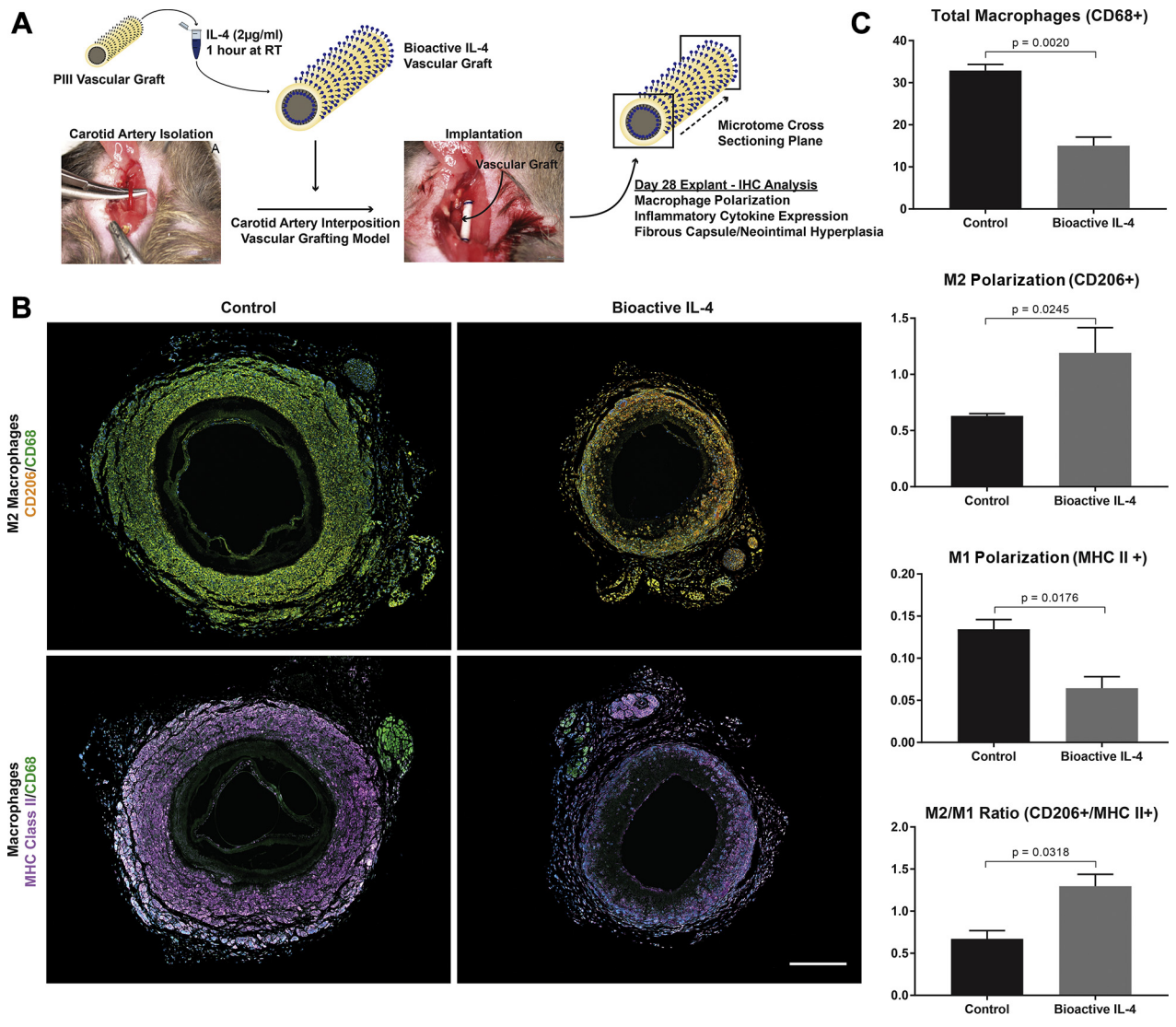

(A) Experimental design schematic; vascular graft dimensions 0.5 mm (inner diameter) × 6 mm length. **(B)** Representative immunostained images of macrophage responses; M2 **(top row)** and M1 **(bottom row)** macrophages. CD68 stained in **green**, CD206 stained in **orange**, and MHC Class II stained in **purple**. Scale bar represents 500 μm. **(C)** Quantification of$CD68^+$ total macrophages **(top)**, $CD206^+$ M2 polarization **(middle)**, MHC Class II^+ M1 polarization, and M2/M1 ($CD206^+$/MHC Class II^+) ratio **(bottom)**. n = 3 slides (each region of the graft) per animal, with a total of 5 animals per group. Abbreviations as in **Figures 1 and 3**.

pro-inflammatory IL-1β and TNF-α expression was 43 ± 9% and 50 ± 3% less in bioactive IL-4 grafts (**Figures 7C and 7D**). Representative images of graft cross-sections demonstrate clear increases in levels of IL-10 and TGF-β, as well as corresponding reductions in IL-1β and TNF-α (**Figure 7E**).

To confirm these findings, qPCR and ELISA analyses were conducted on vascular grafts at days 3 and 7 post-implantation. qPCR results showed that the bioactive grafts had significantly less TNF-α and inducible nitric oxide synthase at days 3 and 7, in addition to reduced CD86 at day 7 (Supplemental Figure 3A). ELISA results supported that bioactive grafts had less IL-1β, IL-6, and TNF-α at day 7 (Supplemental Figure 3B). Consistent with the immunohistochemistry data, these additional results further support our proposed immunomodulatory effects of bioactive surfaces.

In a vascular graft context, inflammatory processes drive both fibrous encapsulation and neointimal

FIGURE 7 Immunohistochemical Analysis of Inflammatory Cytokines in Vascular Grafts

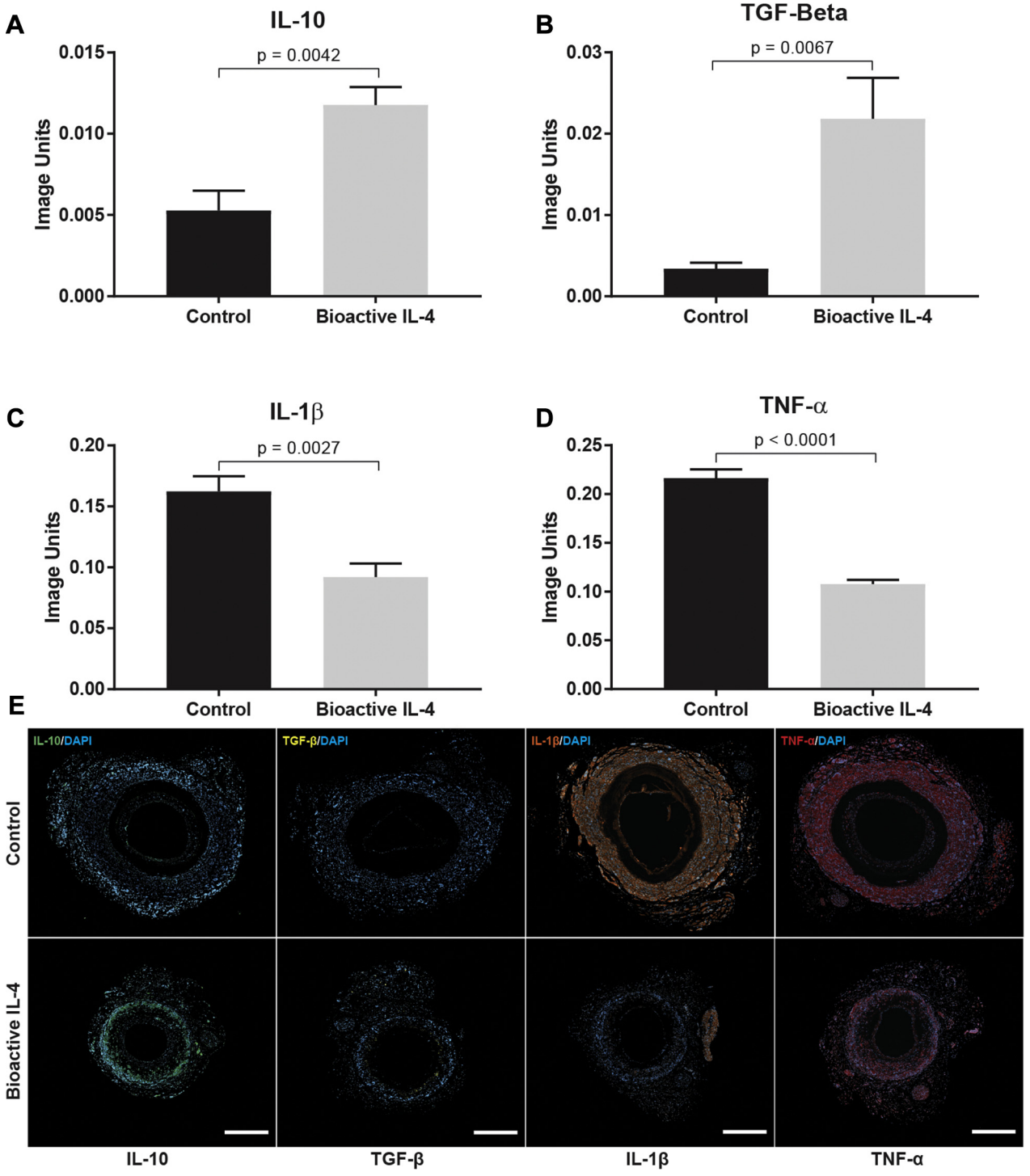

(A) IL-10. **(B)** TGF-β. **(C)** IL-1β. **(D)** TNF-α. **(E)** Representative images of cytokine expression within vascular graft cross sections: control **(top row)** versus bioactive **(bottom row)**. IL-10 stained in **green**, TGF-β stained in **white**, IL-1β stained in **orange**, and TNF-α stained in **red**. Scale bar represents 1 mm; n = 3 slides (each region of the graft) per animal, with a total of 5 animals per group. Abbreviations as in Figures 1 and 4.

FIGURE 8 **Functional Outcomes of Bioactive IL-4 Surfaces for Synthetic Vascular Grafts**

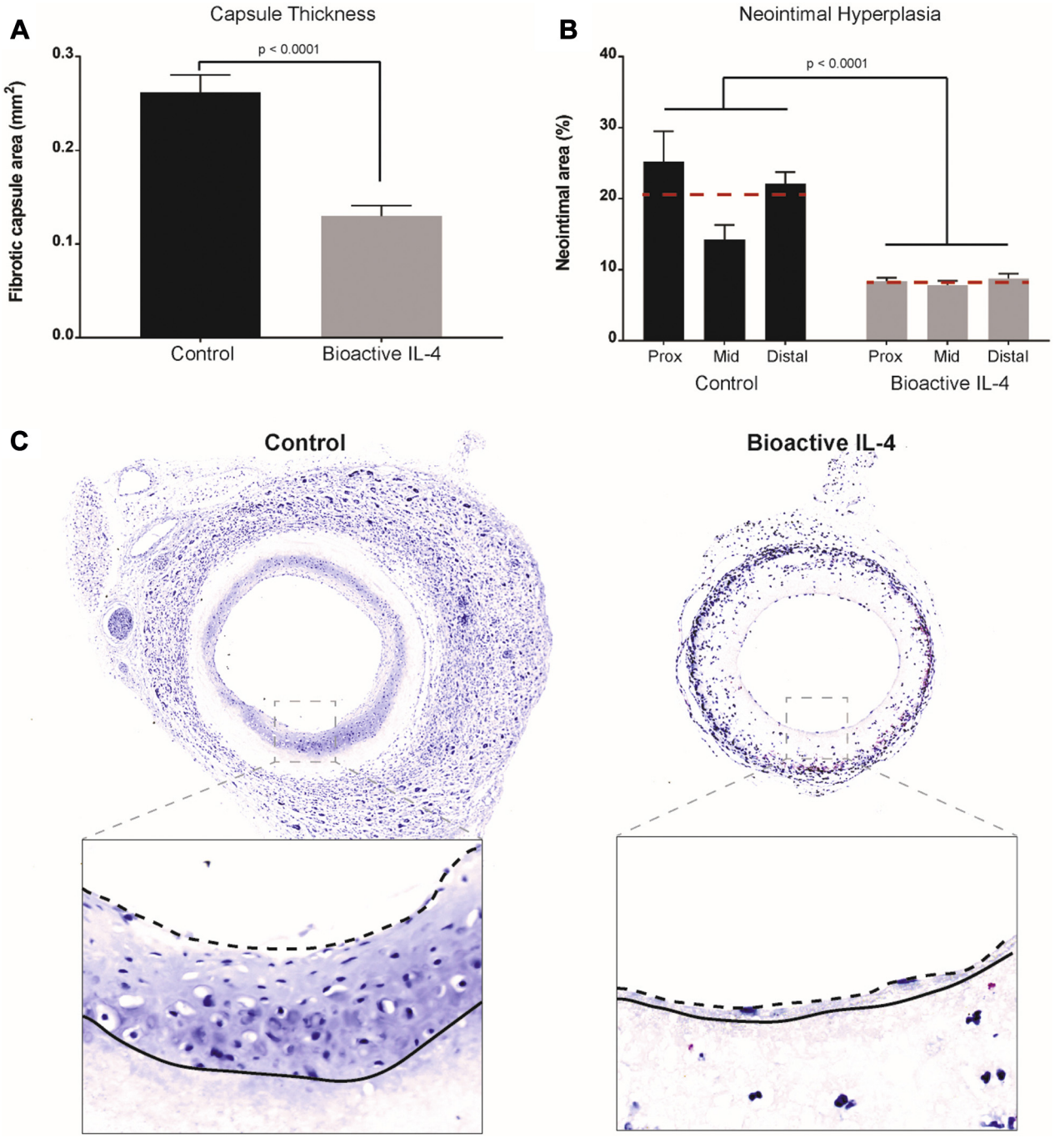

(A) Quantification of adventitia capsule thickness. **(B)** Quantification of neointimal hyperplasia development along 3 segments of vascular graft lumen. **(C)** Representative images of capsule thickness on the adventitia of vascular grafts, scale bar represents 150 μm; representative magnified images of vascular graft lumens **(inset)**. Scale bar represents 40 μm. **Dotted lines** represent the luminal edge of hyperplasia, and **solid lines** represent the luminal graft surface. n = 3 slides (each region of the graft) per animal with the average represented as the **red dotted line**; total of n = 5 animal averages per group. IL-4 = interleukin 4.

hyperplasia leading to graft failure. Adventitial capsule thickness on bioactive IL-4 grafts was 50 ± 1% less than control (**Figure 8A**). In addition, neointimal hyperplasia in bioactive IL-4 grafts was significantly less throughout the length of the graft (**Figure 8B**). The greatest decreases were observed at the proximal and distal anastomoses, with a reduction of 69 ± 6.7% and 61 ± 6.1%, respectively, relative to control. The midsection of the graft also saw significantly less hyperplasia (51 ± 9.6%) compared with control (**Figure 8C**). No significant changes to re-endothelialization were observed between the grafts (Supplemental Figure 4). Further characterization of the neointima observed increases in smooth muscle cells and proliferating cells compared to control while the elastin in the neointima was not significantly different (Supplemental Figure 5). Collectively, these results suggest that local modulation of macrophage phenotypes and cytokine profiles were responsible for significant reductions in neointimal hyperplasia.

DISCUSSION

CAD has become increasingly characterized as a chronic inflammatory disorder, prompting consideration of new anti-inflammatory therapeutic interventions. An overabundance of immune cells is common to atherosclerosis progression and neointimal hyperplasia development. The underlying immune cell presence arises from a complex interplay of inflammatory cytokines, which act to coordinate, propagate, and sustain inflammatory responses. Clinical evidence highlights the therapeutic potential of inhibiting cytokine expression to reduce inflammation and improve outcomes. Although the deployment of cardiovascular materials and devices in high-risk areas is an established treatment for CAD, accelerated inflammatory responses are a major cause of failure (18). In search of the next generation of CAD therapies, there remains an unmet need for cardiovascular devices fabricated from materials capable of modulating local inflammatory responses.

The present study describes rapid resolution of the inflammatory response to implanted materials in 2 separate mouse models, leading to durable functional improvements. Previous studies have shown the feasibility of local modulation of inflammation, using drug release or direct injection approaches to influence cell populations and chemokine profiles (19). Together, these studies have highlighted the limitation of using nonspecific suppressive drugs and the transient effects of these approaches, with most studies showing changes only in the first few days after implantation. Our results show that electrospun PCL scaffolds and conduits can be robustly functionalized with bioactive IL-4 to drive rapid polarization of macrophages to an anti-inflammatory M2 phenotype.

Multiple studies have now reported that implanted materials that promote an early shift to more M2-like macrophages at the material interface have an improved host response. The "alternatively activated" M2 phenotype is driven by signaling from M2-polarizing cytokines, including IL-4 (20). Previous research on IL-4-mediated regulation of the local response to materials has been limited to short-term elution from flat scaffolds. Examples include release from silk scaffolds over 24 h successfully polarizing macrophages in vitro (21) and microsphere-mediated release from poly(lactic-co-glycolic acid) scaffolds that increased the proportion of $CD206^{+}$ macrophages after 1 day in vivo, but local gene expression changes beyond this time were inconsistent (20). Similarly, release of IL-4 from polypropylene meshes showed no change to the number of local macrophages but a shift toward M2 phenotype at 14 days in a mouse subcutaneous implant model (22). Together, these studies illustrate the promise of early-stage macrophage polarization at the tissue implant interface toward an M2 phenotype. However, the applicability of this approach to any functional application, such as in a high-blood flow environment, has yet to be performed.

Robust immobilization of IL-4 onto the surface of PCL substrates was consistent with previous use of PIII surface activation of polymers to immobilize other biomolecules, including fibrillin-1 to polytetrafluoroethylene (PTFE) (23) and tropoelastin to expanded polytetrafluoroethylene (ePTFE) (24) and polyurethane conduits (6). In vitro macrophage interactions with bioactive IL-4 surfaces provided evidence of retained IL-4 bioactivity. The effects of IL-4 immobilization through PIII are consistent with the transient and variable effects on gene expression previously described for eluted IL-4 (20,21). PIII treatment is also well suited to the modification of implanted materials due to the established benefits of a long shelf-life post-treatment and the rapid covalent binding of a range of biomolecules during solution incubation (6). At the bedside, these off-the-shelf features would allow for the preparation of bioactive surfaces by simply taking pre-treated PIII materials/devices off the shelf and immersing them in IL-4

solutions, ready for transplant into patients with minimal time and cost expenditures.

The findings of the present study suggest that simultaneous changes to the local expression of both pro- and anti-inflammatory cytokines may be a more suitable approach to achieve rapid and comprehensive resolution of inflammation. Modulating macrophage phenotype and behavior is potentially an effective way of accomplishing this goal, demonstrating a preferable immunomodulatory strategy in the context of materials for vascular repair. Furthermore, these changes led to functional reductions in fibrous encapsulation sustained for at least 14 days. In contrast, studies using passive release of IL-4 commonly report upregulation of M2 macrophages surrounding implants but typically no significant differences in total cell accumulation (20) or macrophages (22) at the implant interface. In fact, M2 macrophage polarization is greatest at distances farthest from the surface of drug elution, accentuating the disadvantage of passive release strategies in which IL-4 diffuses away from the implant site. Significant reductions in cell accumulation and fibrous encapsulation seen on bioactive IL-4 surfaces demonstrate improved functional outcomes compared with passive release strategies. More broadly, our findings suggest the potential utility for a diverse range of tissue repair applications. Previous studies have highlighted benefits for regulating the inflammatory response to scaffolds in the context of soft tissue and wound repair, as well as potentially in cardiac patches to treat myocardial infarction in which the role of macrophage polarization has recently been highlighted (25). Studies thus far share the limitation of being restricted to analysis in tissue, with none to date modulating inflammation in flowing blood.

The present study reports sustained effectiveness in a vascular graft context with direct implications for vascular materials and devices deployed in contact with circulation. Regulating fibrotic encapsulation is important for limiting compliance mismatch between the graft and adjacent native vasculature, which has long been correlated with poor patency in small-diameter applications (26). Restenosis, the main source of long-term graft occlusion, is caused by neointimal hyperplasia and widely accepted to be inflammation driven. Previous studies have clearly reported this link observing reduced neointima formation after inhibition of leukocyte trafficking (27), release of dexamethasone (28), the cytotoxic drugs paclitaxel and sirolimus (29), and specific anti-inflammatory CX_3CR1 antagonists (30). Although these strategies have collectively shown promising in vitro results, beneficial long-term outcomes in vivo have not been reported, with efficacy often limited to the period of drug elution. In addition to the benefit of immobilization to address these issues, bioactive IL-4 surfaces drive a rapid shift of the native immune response that would be expected to have lasting effects long after the IL-4 biomolecules are removed from the surface. By elevating M2 macrophage populations, yielding favorable modulation of the inflammatory response through regulation of both pro- and anti-inflammatory cytokines, the foreign body response is more quickly resolved. Our research has significant implications for improving the inflammatory response to all implants, with potential applications for cardiovascular devices in contact with flowing blood such as the prevention of foreign body encapsulation and neointimal hyperplasia in small diameter conduits.

STUDY LIMITATIONS. Limitations to this study include the use of a small animal model of grafting, with a nondiseased phenotype, and a short-time frame of neointimal hyperplasia assessment. While the mouse grafting model used in this study facilitates quantification of clinically relevant endpoints such as neointimal hyperplasia and re-endothelialization, the established pre-clinical pathway includes larger animals including sheep. The sheep model more closely resembles human pathology and incorporates additional considerations of graft efficacy including thrombogenicity and longer-term graft performance. The wild-type mice used in this study have a healthy vasculature, lacking the persistent inflammatory environment commonly present in atherosclerosis and CAD. Use of fat-fed or transgenic animals may potentially benefit future studies investigating bioactive vascular grafts in cardiovascular disease phenotypes. The findings of this study justify the further assessment of bioactive IL-4 surfaces in the context of atherosclerosis and in larger animal models with implications for improving the efficacy of all implants, including small diameter vascular grafts.

CONCLUSIONS

The present study evaluated a novel bioactive device coating that modulates macrophage phenotype and extensively suppresses local inflammatory responses. The bioactivity of our surfaces relies on a covalently immobilized layer of IL-4, a key regulator of macrophage recruitment and anti-inflammatory polarization, to provide comprehensive suppression of

inflammation. As a subcutaneous implant, bioactive IL-4 surfaces exhibited increased polarization of macrophages to their anti-inflammatory M2 phenotype, reducing the overall recruitment of macrophages. This finding also correlates with the favorable regulation of inflammatory cytokine production that led to striking reductions in the formation of the foreign body fibrotic capsule at 2 weeks after implantation. Using these materials as vascular grafts, we observed the same striking effects on macrophage reduction, M2 polarization, and positive regulation of the local cytokine environment, which translate to important functional outcomes, most notably a significant reduction in foreign body encapsulation and neointimal hyperplasia development after 1 month in vivo. The collective findings of our 2 models have significant implications for improving the inflammatory response and the long-term performance of medical implants, with demonstrated potential for cardiovascular devices in contact with flowing blood.

ACKNOWLEDGMENTS The authors acknowledge the facilities as well as scientific and technical assistance at the Australian Center for Microscopy and Microanalysis, The University of Sydney.

ADDRESS FOR CORRESPONDENCE: Mr. Richard P. Tan, Applied Materials Group, The Heart Research Institute, 7 Eliza Street, Newtown NSW 2042, Australia. E-mail: richard.tan@hri.org.au.

PERSPECTIVES

COMPETENCY IN MEDICAL KNOWLEDGE: CAD and other manifestations of atherosclerosis have become increasingly characterized as inflammatory disorders. The success of future interventional therapies for CAD requires effective delivery of anti-inflammatory agents that can provide localized and sustained suppression of inflammation while avoiding the adverse effects of systemic administration, including infection. Representing an alternative approach to systemic treatment, this study investigates the targeted delivery of the anti-inflammatory cytokine IL-4 through bioactive coatings on materials capable of being implanted into the vasculature.

TRANSLATIONAL OUTLOOK: Given their roles as major effectors of innate immunity, targeting macrophage phenotype and behavior may represent a more focused and comprehensive approach to immunomodulation, with potentially greater impact on improved cardiac outcomes for implanted vascular materials. Bioactive surfaces with immobilized IL-4 can modulate local inflammation in a sustained and robust manner. These have numerous applications for implants and devices being implanted into high-risk cardiovascular areas, with the immediate benefits of improving device performance as well as the long-term advantages of mitigating chronic inflammation that drive CAD pathology.

REFERENCES

1. Hansson GK. Inflammation, atherosclerosis, and coronary artery disease. N Engl J Med 2005;352:1685–95.

2. Mulvihill NT, Foley JB. Inflammation in acute coronary syndromes. Heart 2002;87:201–4.

3. Ridker PM, Everett BM, Thuren T, et al. Antiinflammatory therapy with canakinumab for atherosclerotic disease. N Engl J Med 2017;377:1119–31.

4. Bridges AW, García AJ. Anti-Inflammatory polymeric coatings for implantable biomaterials and devices. J Diabetes Sci Technol 2008;2:984–94.

5. Hiroyuki O, Tsutomu T, Kiyoshi Y. Therapies targeting inflammation after stent implantation. Curr Vasc Pharmacol 2013;11:399–406.

6. Bilek MM. Biofunctionalization of surfaces by energetic ion implantation: review of progress on applications in implantable biomedical devices and antibody microarrays. Appl Surf Sci 2014;310:3–10.

7. Pajarinen J, Tamaki Y, Antonios JK, et al. Modulation of mouse macrophage polarization in vitro using IL-4 delivery by osmotic pumps. J Biomed Mater Res A 2015;103:1339–45.

8. Kondyurin A, Bilek M. 10—Protection in an aggressive environment. Ion Beam Treatment of Polymers. Amsterdam, the Netherlands: Elsevier, 2008:243–60.

9. Liu H, Wise SG, Rnjak-Kovacina J, et al. Biocompatibility of silk-tropoelastin protein polymers. Biomaterials 2014;35:5138–47.

10. Chan AH, Tan RP, Michael PL, et al. Evaluation of synthetic vascular grafts in a mouse carotid grafting model. PLoS One 2017;12:e0174773.

11. Bilek MM, McKenzie DR. Plasma modified surfaces for covalent immobilization of functional biomolecules in the absence of chemical linkers: towards better biosensors and a new generation of medical implants. Biophysical Reviews 2010;2:55–65.

12. Bilek MM, Bax DV, Kondyurin A, et al. Free radical functionalization of surfaces to prevent adverse responses to biomedical devices. Proc Natl Acad Sci U S A 2011;108:14405–10.

13. Liu CP, Zhang X, Tan QL, et al. NF-κB pathways are involved in M1 polarization of RAW 264.7 macrophage by polyporus polysaccharide in the tumor microenvironment. PLoS One 2017;12:e0188317.

14. Liu CY, Xu JY, Shi XY, et al. M2-polarized tumor-associated macrophages promoted epithelial-mesenchymal transition in pancreatic cancer cells, partially through TLR4/IL-10 signaling pathway. Lab Invest 2013;93:844–54.

15. Li B, Cao H, Zhao Y, et al. In vitro and in vivo responses of macrophages to magnesium-doped titanium. Sci Rep 2017;7:42707.

16. Tan RP, Lee BSL, Chan AH, et al. Non-invasive tracking of injected bone marrow mononuclear cells to injury and implanted biomaterials. Acta Biomater 2017;53:378–88.

17. Anderson JM, Rodriguez A, Chang DT. Foreign body reaction to biomaterials. Semin Immunol 2008;20:86–100.

18. Inoue T, Croce K, Morooka T, Sakuma M, Node K, Simon DI. Vascular inflammation and repair: implications for reendothelialization,

restenosis, and stent thrombosis. J Am Coll Cardiol Intv 2011;4:1057–66.

19. Browne S, Pandit A. Biomaterial-mediated modification of the local inflammatory environment. Front Bioeng Biotechnol 2015;3:67.

20. Minardi S, Corradetti B, Taraballi F, et al. IL-4 release from a biomimetic scaffold for the temporally controlled modulation of macrophage response. Ann Biomed Eng 2016;44:2008–19.

21. Reeves AR, Spiller KL, Freytes DO, Vunjak-Novakovic G, Kaplan DL. Controlled release of cytokines using silk-biomaterials for macrophage polarization. Biomaterials 2015;73:272–83.

22. Hachim D, LoPresti ST, Yates CC, Brown BN. Shifts in macrophage phenotype at the biomaterial interface via IL-4 eluting coatings are associated with improved implant integration. Biomaterials 2017;112:95–107.

23. Hajian H, Wise SG, Bax DV, et al. Immobilisation of a fibrillin-1 fragment enhances the biocompatibility of PTFE. Colloids Surf B Biointerfaces 2014;116:544–52.

24. Wise SG, Liu H, Kondyurin A, et al. Plasma ion activated expanded polytetrafluoroethylene vascular grafts with a covalently immobilized recombinant human tropoelastin coating reducing neointimal hyperplasia. ACS Biomaterials Sci Eng 2016;2:1286–97.

25. Mongue-Din H, Patel AS, Looi YH, et al. NADPH oxidase-4 driven cardiac macrophage polarization protects against myocardial infarction-induced remodeling. J Am Coll Cardiol Basic Trans Science 2017;2:688.

26. Baird RN, Abbott WM. Pulsatile blood-flow in arterial grafts. Lancet 1976;308:948–50.

27. Lavin B, Gomez M, Pello OM, et al. Nitric oxide prevents aortic neointimal hyperplasia by controlling macrophage polarization. Arterioscler Thromb Vasc Biol 2014;34:1739–46.

28. Liu X, De Scheerder I, Desmet W. Dexamethasone-eluting stent: an anti-inflammatory approach to inhibit coronary restenosis. Expert Rev Cardiovasc Ther 2004;2:653–60.

29. Wessely R, Schömig A, Kastrati A. Sirolimus and paclitaxel on polymer-based drug-eluting stents: similar but different. J Am Coll Cardiol 2006;47:708–14.

30. Ali MT, Martin K, Kumar AH, et al. A novel CX3CR1 antagonist eluting stent reduces stenosis by targeting inflammation. Biomaterials 2015;69:22–9.

KEY WORDS covalent biomolecule immobilization, inflammation, interleukin-4, neointimal hyperplasia, plasma-based ion implantation, radical functionalized surface, vascular graft

APPENDIX For supplemental figures, results, and methods, please see the online version of this paper.